JMEPEG (2013) 22:2997–3004
DOI: 10.1007/s11665-013-0589-9

1059-9495/$19.00

Hydroxyapatite-Coated Magnesium-Based Biodegradable Alloy: Cold Spray Deposition and Simulated Body Fluid Studies

Abdullah C.W. Noorakma, Hussain Zuhailawati, V. Aishvarya, and B.K. Dhindaw

(Submitted April 17, 2013; in revised form April 17, 2013; published online May 18, 2013)

A simple modified cold spray process in which the substrate of AZ51 alloys were preheated to 400 °C and sprayed with hydroxyapatite (HAP) using high pressure cold air nozzle spray was designed to get biocompatible coatings of the order of 20-30 µm thickness. The coatings had an average modulus of 9 GPa. The biodegradation behavior of HAP-coated samples was tested by studying with simulated body fluid (SBF). The coating was characterized by FESEM microanalysis. ICPOES analysis was carried out for the SBF solution to know the change in ion concentrations. Control samples showed no aluminum corrosion but heavy Mg corrosion. On the HAP-coated alloy samples, HAP coatings started dissolving after 1 day but showed signs of regeneration after 10 days of holding. All through the testing period while the HAP coating got eroded, the surface of the sample got deposited with different apatite-like compounds and the phase changed with course from DCPD to β-TCP and β-TCMP. The HAP-coated samples clearly improved the biodegradability of Mg alloy, attributed to the dissolution and re-precipitation of apatite showed by the coatings as compared to the control samples.

Keywords bioactivity, biodegradability, cold spray deposition, hydroxyapatite, magnesium alloy, SBF study

1. Introduction

In the commonly used implant materials such as Ti-6Al-4V, stainless steel, and Co-Cr alloys, release of toxic metal ions into the body and their adverse effects on the host over a period of time is well documented (Ref 1). Increased concern over the toxicity of metallic implants led to development of biodegradable implants and biocompatible coatings on implant materials.

The biodegradable implants can gradually be dissolved, absorbed, consumed, or excreted. Magnesium has been suggested as an alternative biomaterial recently due to its easy degradability and near equivalent mechanical properties to that of bone. The strong points in favor of using magnesium as implant are strongly fortified by the their attractive biological performances (Ref 2, 3): (1) metal magnesium is biodegradable in body fluid by corrosion; (2) Mg^{2+} is an essential element to the human body (the daily intake of Mg^{2+} for a normal adult is 300-400 mg) and hence harmless; (3) Magnesium can accelerate the growth of new bones tissues; (4) Density, elastic modulus, and yield strength of magnesium are closer to the bone tissue than that of the conventional implants (Ref 2, 3).

Despite its excellent properties magnesium-based alloys have not seen tangible applications in biomedical implant industry (Ref 4). To date magnesium and its alloys have been studied in the development of cardiovascular stents, bone fixation material, and porous scaffolds for bone repair (Ref 4-6). Nevertheless, the main limitation to the medical application is their corrosion behavior. Corrosion occurs rapidly even for a biodegradable material and additionally, it is not homogenous due to the tendency for localized corrosion (Ref 7). Another issue raised is related to the formation of hydrogen during corrosion. In the case of high evolution of hydrogen gas, magnesium cannot be absorbed in the body and a balloon effect takes place. In addition, an alkaline pH shift in the vicinity of corroding surface that is also a concern for medical applications. Therefore, it is necessary to carry out surface treatment or form coatings (Ref 8). The coatings enable biodegradation at controlled rate, and hence they offer a limited barrier function.

In order to control the degradation rate that can be extremely rapid to Mg alloy, it is useful to coat with hydroxyapatite (HAP). The HAP $[Ca_{10}(PO_4)_6OH_2]$ is a form of calcium apatite and is the major component that is composed of same ions responsible to construct the mineral part of bone and teeth. HAP is bioactive with bone bonding ability, clinically used as bone spacers and fillers. The lack of cytotoxic effect makes HAP biocompatible with hard tissue and soft tissue (Ref 9). HAP helps to improve the biodegradation rate of magnesium alloys.

Abdullah C.W. Noorakma, School of Materials and Mineral Resources Engineering, Universiti Sains Malaysia, 14300 Nibong Tebal, Pulau Pinang, Malaysia, and now Faculty of Design and Engineering Technology, Universiti Sultan Zainal Abidin, 21300 Kuala Terengganu, Malaysia; **Hussain Zuhailawati,** School of Materials and Mineral Resources Engineering, Universiti Sains Malaysia, 14300 Nibong Tebal, Pulau Pinang, Malaysia; **V. Aishvarya,** Surface Engineering Department, Institute of Minerals and Materials Technology, Council of Scientific & Industrial Research (CSIR), Bhubaneswar 751013, India; and **B.K. Dhindaw,** Indian Institute of Technology, Bhubaneswar, 604, A Block, Toshali Bhawan, Satyanagar, Bhubaneswar 750015, India; Contact e-mails: wan_noorakma@yahoo.com, zuhaila@eng.usm.my, aishvarya@immt.res.in, dhindaw@metal.iitkgp.ernet.in.

Recently, some research works were performed to slow down the biodegradation rate of magnesium alloys, including sol gel (Ref 1) electrodeposition (Ref 2). Among them, plasma spraying of magnesium alloys has not been widely investigated possibly due to the low melting temperature of magnesium. Additionally, when HAP is plasma sprayed, it may be converted into other calcium phosphate phases such as α- or β-tricalcium phosphate, tetracalcium phosphate (TTCP), or calcium oxide (CaO) and the crystallinity of HAP may also be lowered due to rapid solidification. These alterations in chemistry and crystallinity often interfere with the novel bioactive properties of HAP as well as its adhesion to the implant (Ref 9, 10).

In this study, we demonstrate a novel approach to coat the HAP on AZ51 magnesium alloy by the modified cold spray (CS) deposition technique. AZ51 was chosen as experimental alloy to investigate the biodegradation of magnesium coated with HAP. Since the coated samples were meant for specific applications where time bound healing should start before the whole implant dissolves, regeneration of HAP from the SBF solution was studied in particular to examine the bioactivity of the coating.

To investigate the effect of HAP coating by the above technique, dissolution study was conducted to find the bioactivity when subjected to the physiological medium. The biodegradation rate of AZ51 coated with HAP by cold-sprayed coating technique was evaluated in the simulated body fluid (SBF).

2. Materials and Methods

2.1 Materials

The substrate material was AZ51 (5% Al, 1% Zn) magnesium alloy plate. The alloy was obtained from GKSS research center, Germany. The specimens were cut into small pieces with 15 mm × 15 mm × 4 mm. The specimens surface were ground with 1000 grit SiC paper to ensure the same surface roughness. Then the specimens were ultrasonically cleaned in acetone for 5 min. HAP, $Ca_5OH(PO_4)_3$ (purum p.a., ≥ 90%) powder supplied by Sigma Aldrich were used as spray-dried materials. The average particle size of powder was 4 μm. The as-received HAP powder was characterized with Bruker AXS D8 XRD unit using a monochromatic Cu Kα radiation at a scan rate of 0.04 degree/s in the range of 20°-60° angle. XRD result of the as-received HAP powder indicated the characteristic peaks of pure HAP (Fig. 1). The crystallographic structure of HAP was hexagonal with *P*63/*m* space group. The lattice constant was, a = 9.424 Å and matched with the reference pattern file no. 01-074-0565 (ICDD).

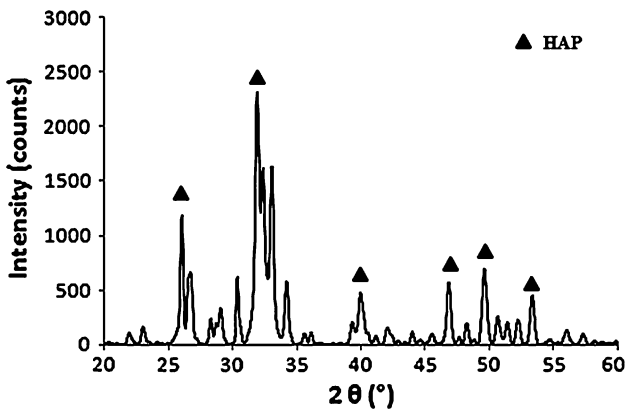

Fig. 1 XRD pattern of as-received HAP powder

2.2 Preparation of HAP Coatings

In conventional CS technique hot gases at temperatures 500-700 °C is used as carriers of the sprayed powders while the substrate remains at room temperature. In the present study, the CS technique was modified by using ambient air at room temperature as the spraying medium and heating the substrate to 400 °C. This modification helped in retaining the HAP properties which usually show phase changes at high temperature deposition. HAP coating was prepared by placing the AZ51 substrate inside a furnace where it was preheated to a temperature of 400 °C for 1 h. After the substrate was heated for 1 h, the HAP powder was sprayed using the modified CS deposition system. In this process the HAP powder was deposited on preheated substrate by high pressure powder feeder through an air spraying nozzle. The nozzle was kept 40 mm from the preheated substrate. The spraying HAP powder was accelerated to a high velocity and deposited on the heated AZ51 substrate. The air pressure was 10 bars and was controlled at room temperature.

2.2.1 Characterization of HAP Coatings and SBF Solution. The surface morphology, deposit thickness, and the composition of as-deposited coating and test samples were studied by field emission scanning electron microscopy Zeiss SUPRA 35VP (FESEM) from Germany, equipped with energy dispersion x-ray spectrometry (EDX). EDX was carried out at a voltage of 15 kV and a working distance of 10 mm, while morphology was studied at 5 mm working distance and 5 kV. Surface topography of coatings was examined by atomic force microscope (AFM). The AFM model was NanoNavi SII from Japan.

The hardness and elastic modulus of the coating were evaluated by the Nanoindentation test. Nanoindentation was performed using Nano Test Instrument (Micro Materials Ltd Wrexham, UK). Three different loads were used: 10, 100, and 300 mN. The indentations were conducted using the load control mode, where the load is applied and then released after the set peak. An initial load of 0.05 mN was used for locating the surface with Berkovich indenter. After this a loading rate of 10% of the load was applied. A dwell time of 5 s was applied at the maximum load.

The calcium, phosphorous, and magnesium ions concentration in the solution were analyzed immediately after the specimens were removed from SBF solution using the Perkin Elmer 8300 inductively coupled plasma optical emission spectroscopy (ICPOES), USA. All the SBF test solutions were appropriately diluted in de-ionized water and subjected to ICPOES analysis.

2.3 Studies with SBF

SBF was prepared as described by Kakubo et al. (Ref 11) by dissolving reagent grade NaCl, $NaHCO_3$, KCl, $K_2HPO_4{\cdot}3H_2O$, $MgCl_2{\cdot}6H_2O$, $CaCl_2$, Na_2SO_4, in ion exchanged and distilled water. The synthesized solution was buffered at pH 7.30 ± 0.05 with Tris-hydroxymethyl aminomethane, $(HOCH_2)_3CNH_2$, and 1 M HCl. All chemicals used in this study were of analytical reagent grade obtained from Sigma Aldrich, USA.

The volume of the SBF solution for soaking the specimen was determined by the formula $V_s = S_a/10$ where the V_s is the volume of the SBF (Ml) and S_a is the apparent surface area of

the specimen (mm^2) (Ref 11). The calculated volume of SBF was put into plastic container and was heated at 36.5 °C. The specimens were placed in the SBF after the solution attained a temperature of 36.5 °C. Uncoated AZ51 specimens were used as control sample henceforth mentioned as 'Control', to check the biodegradation effect of SBF on pure alloy.

The control and coated AZ51 specimens were soaked in the SBF solution for various periods of 1, 4, 10, and 14 days. The solution pH was monitored during the immersion period using a 3-point calibrated pH electrode (SYSTRONICS 362). After reaching the immersion time, the specimens were taken out for analysis from SBF solution and gently rinsed with pure water. The experiments were carried out at 37 °C in the water bath. The test tubes were sealed to remain sterile. The specimens were dried in desiccators without heating. In the same test tube it was not possible to place several samples, as the change in the chemistry of the solution due to each sample would interfere with the dissolution characteristics of the other samples. Thus one sample could only be placed in one test tube.

3. Result and Discussion

3.1 Surface Morphologies and Chemical Analysis of HAP Coatings

Figure 2(a) and (b) shows the SEM micrograph depicting the surface morphology and the structure of HAP coating on the samples. SEM micrograph clearly showed that a dense HAP coating was deposited on AZ51 plate. Based on this microstructure, the HAP particles were found to be bonded well to each other during the CS process. Possibly higher impact velocity of HAP particles in conjunction with the heat from AZ51 substrate might have caused the particles to bond with each other. Figure 2(c) shows the cross-sectional view of the coating. The film thickness ranged 20-30 μm with an average value of 25 μm and was nearly uniform. The SEM microanalysis with EDX spectra on the coating surface showed that the main elements in the coating were Ca, P, and O with a weight percentage in the range of HAP composition. At the interface with the substrate Ca, P, O, and Mg were observed. Some dark voids were seen at the interface zone. These may have formed due to the deposition process. Since the aim of this study was not to allow dissolution of the complete coating till the interface, the characterization of the interface was not pursued further.

XRD pattern of the coatings showed similar peak as placed in Fig. 1 (not shown). This result indicated that the modified CS technique did not change the character of the HAP phase in the coating deposited on the heated AZ51 substrate.

3.2 Surface Topography of HAP Coatings

Surface topography of the HAP coating surface was visualized by the AFM. Figure 3 shows the AFM image of coating. From this figure it is seen that the coating roughness was uniform and the size of the smallest HAP particle in the agglomerate was about 40 to 60 nm. Agglomeration can be seen in some areas of the topography image. The variation in color in different regions is due to variation in signal with depth

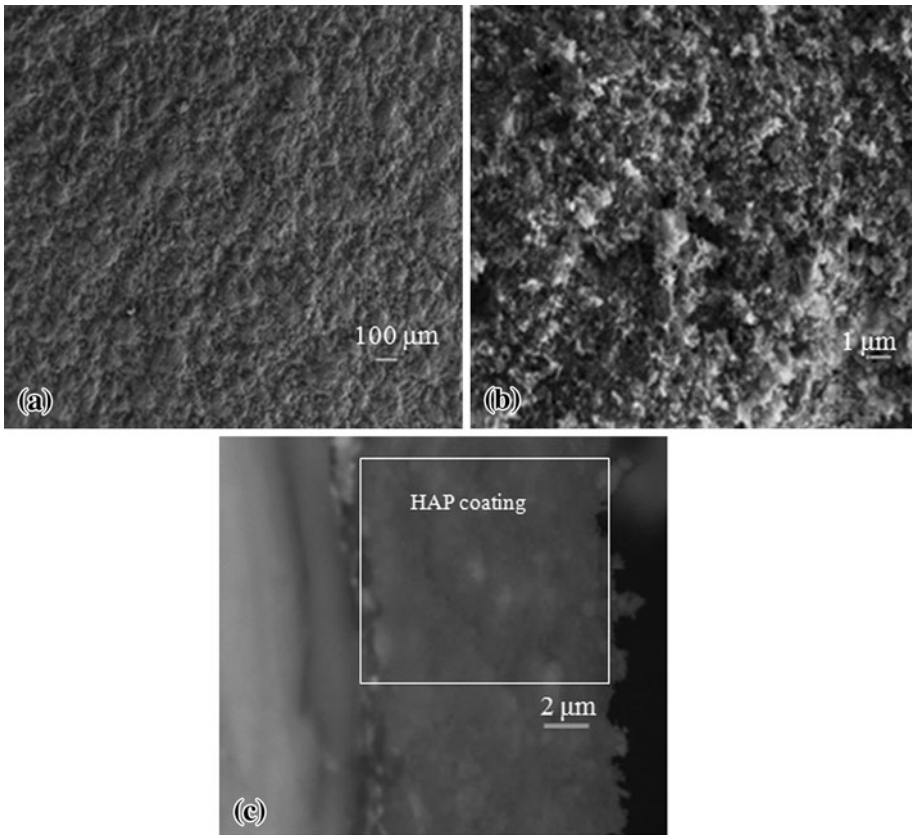

Fig. 2 SEM micrograph of HAP coating on the sample (a) low magnification, (b) high magnification, (c) cross-sectional view

which corresponds to the height difference or roughness of sample.

3.3 Hardness and Elastic Modulus of Coatings

The hardness of the coating using nano indenter was determined at four points. Three different loads were applied in these tests: 10, 100, and 300 mN. The average hardness values obtained were calculated and plotted against load as presented in Fig. 4(a).

Average hardness of HAP coating obtained was 0.1 GPa for the minimum load of 10 mN. The applied load 10 mN caused the penetration depth of 2275 nm (Fig. 4b). As the load increased to 100 mN with penetration of 9346 nm, the hardness obtained was comparable to that obtained under 10 mN applied load. At 300 mN with maximum depth of 12,460 nm, the hardness obtained was 0.09 GPa. Based on these readings, it can be concluded that the hardness was more or less uniform within the HAP coating. However, within the HAP coating, the hardness slightly increased towards the surface of the coating. Similar observations, in different system, were also reported by Samandari et al. (Ref 12) using plasma spray process to coat HAP on the Ti substrate. The hardness increased from the substrate to the surface (Ref 12).

The average elastic modulus of HAP coating was in the range of 9 GPa as seen in Fig. 4(c). A gradual increase of elastic modulus reading within the coating towards the surface was observed. At the lowest load applied for indentation coating showed the highest elastic modulus value. The elastic modulus of HAP coating was found to be greater than polymeric material like polystyrene but little lower than lead (Ref 13). These values are also similar to hardness of the cold compacted iron powder (Ref 14).

3.4 Biodegradable Behaviors of HAP-Coated Samples

In the SBF studies, dissolution and mineralization of the coating are the two main processes that occur. It was observed in the present experiments that the dissolution and mineralization in the HAP coating varied with the soaking time, as well as the changing ion concentration in SBF.

Figure 5 shows the SEM micrograph of the control sample at different time after immersion in SBF. From the morphology of control sample it is seen that cracks were visible after day 1 (Fig. 5a) with tiny pits formation which grew deeper with time (Fig. 5b, c) towards the end of experiment. The control sample showed significant corrosion in the SBF as expected. Table 1 shows the magnesium content on the surfaces of the control samples. Dissolution of Mg into the SBF in the control sample is evident from the decreasing weight percentage (94 to 52.9%) of Mg on the sample surface. Other than magnesium the elements present in the surface were O, Cl, P, Ca in varying proportions. This could mean that Mg was precipitated as magnesium hydroxide or magnesium chloride on the surface. Magnesium hydroxide acts as a passive protective layer under alkaline conditions which is why the Mg does not completely dissolute into SBF (Ref 15). The corrosion could therefore be due to $MgCl_2$ formation which causes pit nucleation on the surface as reported by Hornberger et al. (Ref 15).

Figure 6 shows the change in morphology of HAP-coated test samples at different time after immersion in SBF. Figure 6(a) shows that the HAP coating on the test samples started dissolving after the first day of immersion. The EDX analysis of the coated test samples and the ICP analysis of the SBF solution after immersion are given in Tables 2 and 3,

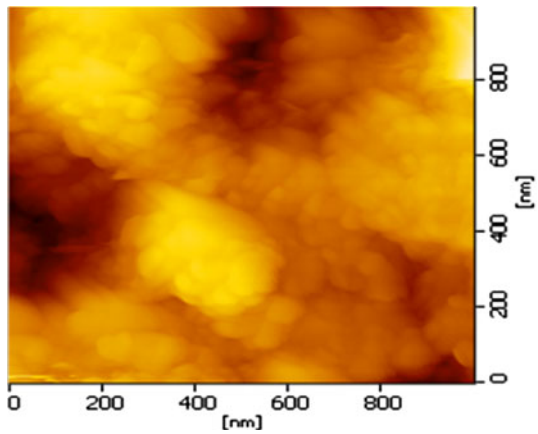

Fig. 3 Two-dimensional AFM image of coated AZ51

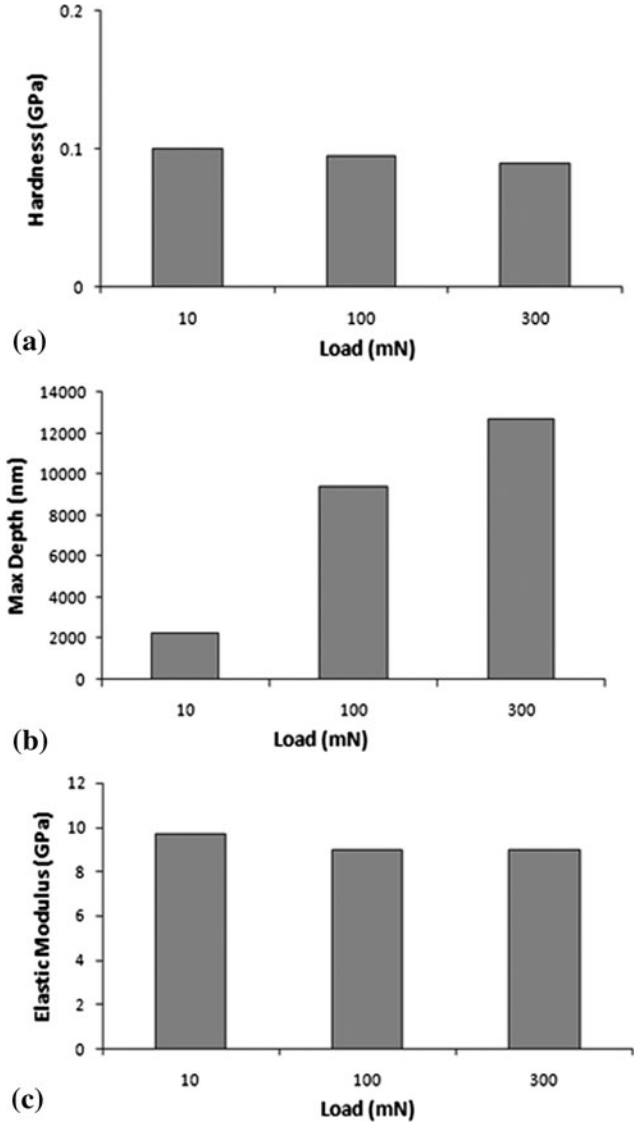

Fig. 4 (a) Hardness of HAP coating at different applied loads, (b) maximum depth of penetration vs. applied load, (c) elastic modulus of HAP coating

respectively. Table 2 shows that there is a general decrease in Mg and fluctuations in the weight percentage of Ca and P elements. The ICP analysis of the SBF solution showed a corresponding increase in Mg and fluctuating Ca and P contents (Table 3). Aluminum did not corrode into SBF and was not detected in ICP analysis. This is beneficial as aluminum corrosion is reported as adverse for bone growth (Ref 3, 4) and the AZ51 alloy shows stability with aluminum. The surface of the coated samples became rough with some loose particles dispersed over the surface. A similar phenomenon was reported for HAP/Ti alloy composite coating deposited by plasma spray on Ti-6Al-4V substrate after soaking in the SBF solution by Gu et al. (Ref 16). It was proposed that this increase in surface roughness of the coating provided nucleation sites and lowered interface energy for bone apatite to anchor (Ref 16).

After 4 days of immersion, the ICP analysis of the solution (Table 3) and the surface morphology of the sample showed significant changes (Fig. 6b). The surface appeared porous and the structure was different from initially seen loose particles on the surface. ICP analysis of SBF showed that there was 10 times reduction in P content with marginal decrease in Ca compared to the first day immersion data. This point out that apatite nucleated on the substrate from solution, probably not noticeable in the SEM image (Fig. 6b), even when corrosion reaction took place.

Figure 6(c) shows the surface morphology of the coating after 10 days of immersion. It was seen that the surface of coated sample was covered by some newly formed layer consisting of small granular agglomerates. The EDX analysis of the agglomerates on the coating showed the presence of Ca, P, O, and Mg, indicating that the granular agglomerate is apatite. However, the weight of Ca element was low on surface and correspondingly high in SBF solution indicating that only little amount of apatite has formed. Chemical analysis of the solution at this stage by ICP showed that Mg content increased over day 4 while P decreased marginally (Table 3). However the small increase in Ca in SBF does not totally preclude the formation of apatite in isolated areas in the film. This confirms that the coating is bioactive, inducing apatite formation.

At the end of 14 days of immersion in SBF, the microanalysis of the coating showed an increase in Ca (Table 2). ICP analysis of the SBF solution complemented this result showing considerable reduction in Ca and a very marginal increase in P (Table 3). Possibly isolated precipitation of apatite on the surface coating might be forming with dissolution still continuing in some other areas. This is also visible in the SEM micrograph as precipitated zone (Fig. 6d). There was a significant reduction in the magnesium content in the SBF (Table 3) meaning dissolution rate slowed down, but was still faster than rate of apatite formation. The SEM micrograph of

Table 1 Change of magnesium concentration on control sample surface during the period of immersion in SBF solution (based on EDX data)

Immersion time, days	0	1	4	10	14
Magnesium on surface, wt.%	94	52.9	52.6	61.2	52.6

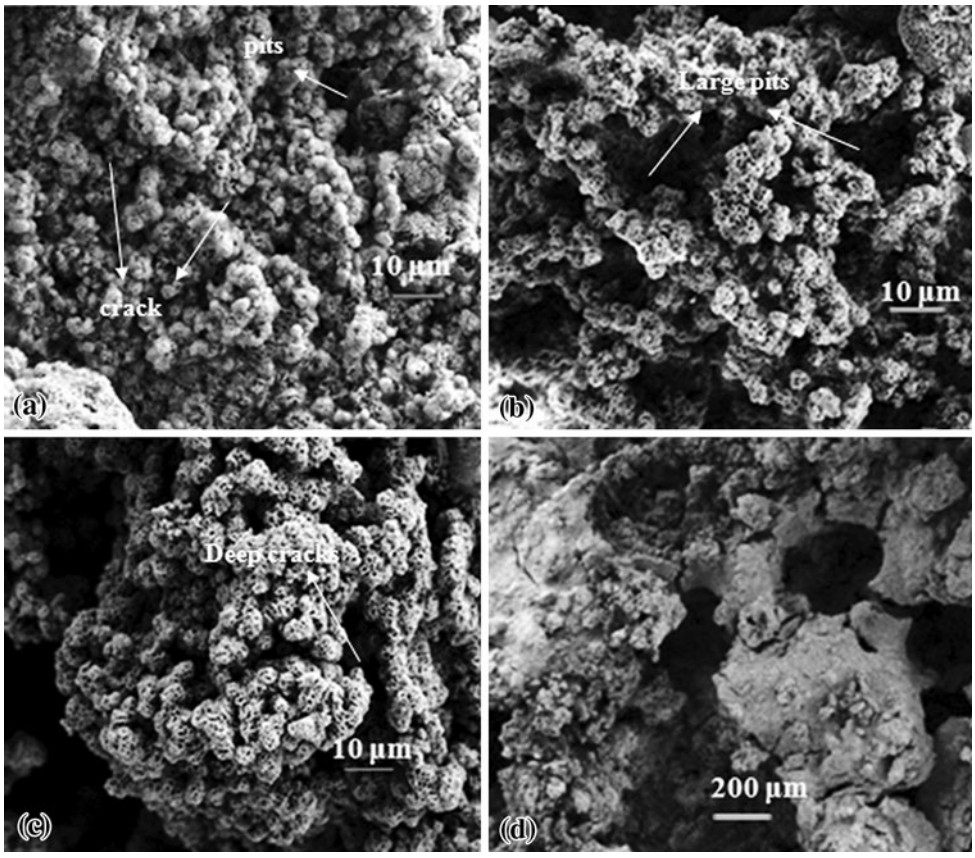

Fig. 5 Surface morphology of control sample showing pit formation (a) after 1 day, (b) after 4 days, (c) after 10 days, and (d) after 14 days of immersion in SBF during in vitro test

the surface after 14 days shows the existence of large size pores and microcracks. It is speculated that the degradation process started happening at the end that caused the damage to the surface structure of the coating. The EDX analysis also showed that 1.2 wt.% Cl was present on the surface at this stage. This indicated that magnesium chloride formation could have initiated.

The pH curve (Fig. 7) shows that the final pH was 8.96 at the end of the incubation period. In the test sample, the pH increase is slower as compared to control sample till day 4. Control sample reaches maximum pH (8.96) after first day of immersion thereafter remains stable. Based on the conditions that prevailed, it is possible to estimate what phase of calcium orthophosphate could have precipitated on the surface, from EDX, ICPOES, and pH data (Ref 17-19). As reported earlier the mechanical properties of the CS coatings were not high enough to make them amenable to analytical procedures including making thin films for TEM micro-diffraction analysis, that involved intense abrasion and cutting procedures. Thus results of EDX analysis along with results from ICPOES were used to semi-quantitatively evaluate the behavior of the precipitating products on the surface. Comparison with similar other works available in the literature were invoked to further substantiate the analysis. To evaluate the dissolution and re-precipitation of apatite, ICPOES data (Table 3) and EDX data (Table 2) are rationalized by calculating the Mg/Ca and Ca/P ratios respectively. The phase of re-precipitated apatite changed through the course of the

Table 2 Change of elemental composition in HAP-coated test samples during the period of immersion (based on EDX data)

Time, days	Ca, wt.%	P, wt.%	Mg on surface, wt.%	Molar Ca/P on substrate
1	0.58	2.05	64.26	0.212
4	0.82	1.89	58.73	0.325
10	0.34	3.45	51.16	0.0739
14	1.16	0.91	54.0	0.956

Table 3 ICPOES analysis of SBF solution after immersion of HAP-coated AZ51 test samples

Immersion time, days	Ion concentration in SBF solution, mg/L			Molar Mg/Ca in solution
	Mg	Ca	P	
0	50.9	158.6	35.1	0.535
1	55.3	162.2	44.6	0.568
4	3906	158.7	4.4	41.02
10	4471	182.8	3.6	40.76
14	3369	149.3	4.2	37.61

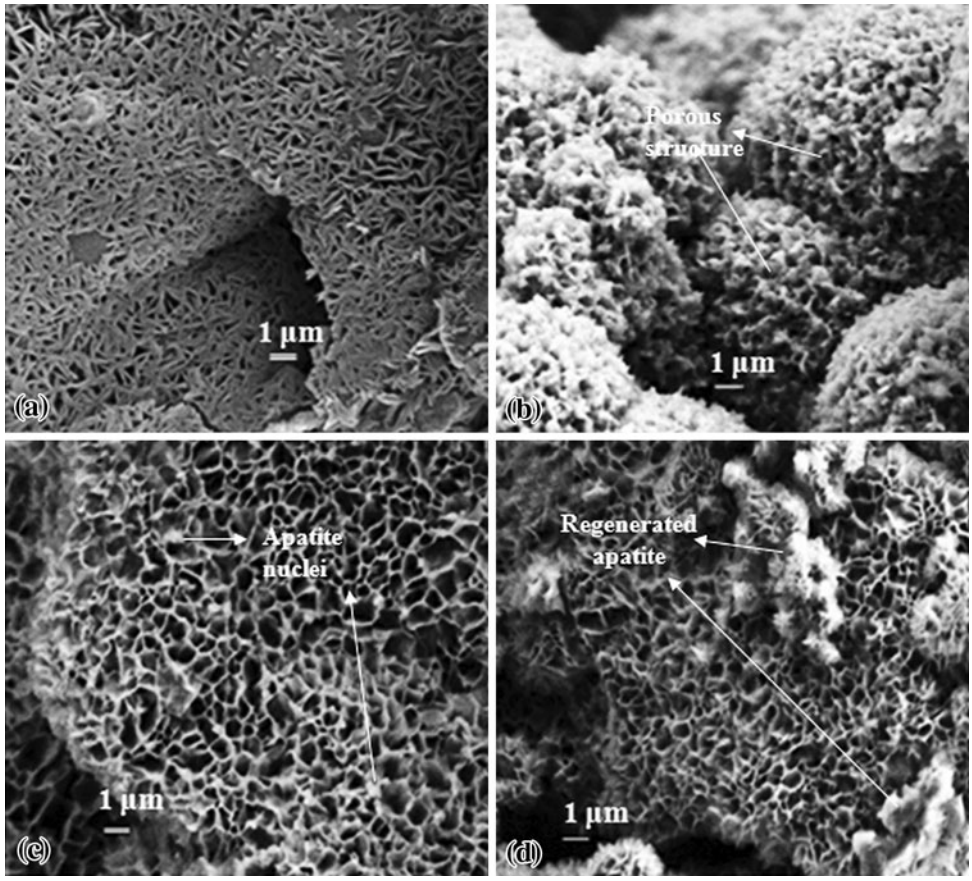

Fig. 6 Surface morphology of HAP-coated samples (a) after 1 day, (b) after 4 days, (c) after 10 days, and (d) after 14 days of immersion in SBF. Initial degradation (a, b) and isolated re-precipitation (c, d) of apatite is visible

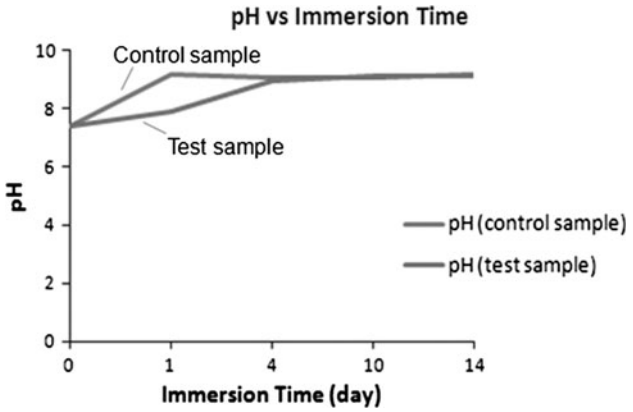

Fig. 7 pH trend of control and test samples during the in vitro experiment

experiment. The molar Ca/P ratio of original SBF solution before the beginning of the experiment is 1.514 (not mentioned in table). From the final molar Ca/P value of 0.956 on day 14 (Table 2), it can be said that the regenerated phase is possibly dicalcium phosphate dihydrate (DCPD). But pH conditions favor β-TCP or β-TCMP formation, which is ideally precipitated in pH range of 5-9 and temperature range of 25-95 °C. Under the same conditions, presence of Mg^{2+} ions in the solution above a ratio of 0.4 with respect to Ca^{2+}, allows biologic or synthetic Mg-substituted TCP formation (Ref 17). The molar Ca/P value and the Mg/Ca values as shown in Tables 2 and 3, respectively, are 0.956 and 37.6 at a pH of 8.96. These values match the conditions said by LeGeros et al. (Ref 18). Hence considering the influence of mildly alkaline pH along with the molar ratios, β-TCMP or Mg-TCP is the most probable phase formed (Ref 17, 18). The stability of both β-TCMP and Mg-TCP in body conditions is little low compared to HAP under physiologic conditions (Ref 19-21), but they act as precursor to the biologic apatite (which is associated with minor but important component such as CO_3 and Mg) as they easily substitute Ca and PO_4 and form calcium-deficient apatite (the naturally occurring apatite) (Ref 17, 22). Due to their faster degradability compared to HAP, β-TCP itself is being used as bone graft substitute and in dental applications allowing faster natural bone growth, a problem encountered with HAP causing prolonged bone growth periods (Ref 18, 21). The re-precipitated phase in the present study is possibly a suitable bioactive material for implant purpose. This is one of the key observations of the present work. Hence with the present rate of biodegradation and bioactivity, the material is suitable for any biodegradable implant application including stents and bone implants. Further in vitro studies of the HAP-coated AZ51 alloy with cell lines can confirm this potential application.

4. Conclusion

A simple and effective CS processing route has been used to prepare HAP coatings on magnesium alloy samples. The coating characterization by SEM confirmed the presence of compact HAP coating on the sample without any phase change during the modified processing. The average thickness of the coating was 25 μm. The smallest aggregates in the coating observed were in the size range of 40-60 nm. Hardness and elastic modulus measured by nano-indentation were found to be around 0.1 and 9 GPa, respectively, indicating that the inter-molecular forces in the coatings are in the high end range of polymers and slightly below metallic lead. SBF tests carried out using SBF solution showed that the HAP coating started dissolving after 1 day of holding and showed signs of regeneration after 10 days. The phase of re-precipitated apatite changed through the course of experiment due to the influence of pH, molar Ca/P and Mg/Ca ratios in solution. At the end of the experiment the apatite re-precipitated as β-TCMP due to increase in pH and favorable change in molar Ca/P and Mg/Ca ratios. The uncoated control samples showed considerable degradation from the very first day onwards of the immersion period. These findings show that the coated alloy is both biodegradable and bioactive, suitable for possible use as biodegradable orthopedic implants.

References

1. S. Shadanbaz and G.J. Dias, Calcium Phosphate Coatings on Magnesium Alloys for Biomedical Applications: A Review, *Acta Biomater.*, 2012, **8**, p 20–30
2. Y.W. Song, D.Y. San, and E.H. Han, Electrodeposition of HAP Coating on AZ91D Magnesium Alloy for Biomaterial Application, *Mater. Lett.*, 2008, **62**, p 3276–3279
3. G.L. Song, Recent Progress in Corrosion and Protection of Magnesium Alloy, *Adv. Eng. Mater.*, 2005, **7**, p 563–586
4. F. Witte, N. Hort, C. Vogt, S. Cohen, K.U. Kainer, R. Willumeit, and F. Feyerabend, Degradable Biomaterials Based on Magnesium Corrosion, *Curr. Opin. Solid State Mater. Sci.*, 2008, **12**, p 63–72
5. R. Zeng, W. Dietzel, F. Witte, N. Hort, and C. Blawert, Progress and Challenge for Magnesium Alloys as Biomaterials, *Adv. Eng. Mater.*, 2008, **10**, p B3–B14
6. F. Witte, The History of Biodegradable Magnesium Implants: A Review, *Acta Biomater.*, 2010, **6**, p 1680–1692
7. S. Hiromoto and M. Tomozawa, HAP Coating of AZ31 Magnesium Alloy by a Solution Treatment and Its Corrosion Behavior in NaCl Solution, *Surf. Coat. Technol.*, 2011, **205**, p 4711–4719
8. J.E. Gray and B. Luan, Protective Coatings on Magnesium and Its Alloys—A Critical Review, *J. Alloys Compd.*, 2002, **336**, p 88–113
9. A. Choudhuri and P.S. Mohanty, Bioceramic Composite Coating by Cold Spray Technology, *Proceedings of the International Thermal Spray Conference*, 2009, p 391–396
10. J. Weng, Q. Liu, J.G.C. Wolke, X. Zhang, and K.D. Groot, Formation and Characteristics of the Apatite Layer on Plasma-Sprayed HAP Coatings in Simulated Body Fluid, *Biomaterials*, 1997, **18**, p 1027–1035
11. T. Kokubo and H. Takadama, How Useful is SBF in Predicting In Vivo Bioactivity?, *Biomaterials*, 2006, **27**, p 2907–2915
12. S.S. Samandari and K.A. Gross, Nanoindentation Reveals Mechanical Properties Within Thermally Sprayed HAP Coatings, *Surf. Coat. Technol.*, 2008, **203**, p 1660–1664
13. B.J. Briscoey, L. Fiori, and E. Pelillo, Nano-indentation of Polymeric Surfaces, *J. Phys. D: Appl. Phys.*, 1998, **31**, p 2395–2405
14. D. Poquillon, V. Baco-Charles, P. Tailhades, and E. Andrieu, Cold Compaction of Iron Powders-Relations Between Powder Morphology and Mechanical Properties, Part II. Bending Tests: Result and Analysis, *Powder Technol.*, 2002, **126**, p 75–84
15. H. Hornberger, S. Virtanen, and A.R. Boccaccini, Biomedical Coatings on Magnesium Alloys—A Review, *Acta Biomater.*, 2012, **8**, p 2442–2455
16. Y.W. Gu, K.A. Khor, and P. Cheang, In Vitro Studies of Plasma-Sprayed HAP/Ti-6Al-4V Composite Coatings in Simulated Body Fluid (SBF), *Biomaterials*, 2002, **24**, p 1603–1611

17. R.Z. LeGeros, Calcium Phosphates in Oral Biology and Medicine, *Monographs in Oral Sciences*, Vol 15, H. Myers, Ed., Karger, Basel, 1991,
18. R.Z. LeGeros, A.M. Gatti, R. Kijkowska, D.Q. Mijares, and J.P. Legeros, Mg-Substitutes Tricalcium Phosphates: Formation and Properties, *Key Eng. Mater.*, 2004, **254–256**, p 127–130
19. J.C. Ellliott, *Structure and Chemistry of Apatites and Other Calcium Orthophosphates*, Elsevier, Amsterdam, 1994, p 137–138
20. L. Cleries, J.M. FernalHndez-Pradas, and J.L. Morenza, Behavior in Simulated Body Fluid of Calcium Phosphate Coatings Obtained by Laser Ablation, *Biomaterials*, 2000, **21**, p 1861–1865
21. A. Priya, S. Nath, K. Biswas, and B. Basu, In Vitro Dissolution of Calcium Phosphate-Mullite Composite in Simulated Body Fluid, *J. Mater. Sci. Mater. Med.*, 2010, **21**, p 1817–1828
22. R.Z. LeGeros, Apatites in Biological Systems, *Prog. Cryst. Growth*, 1981, **4**, p 1–45